

**Ligand-Dependent Ag<sub>2</sub>S Formation: Changes in Deposition  
of Silver Nanoparticles with Sulfidation**

Journal:	<i>Environmental Science: Nano</i>
Manuscript ID	EN-COM-12-2017-001240.R1
Article Type:	Communication
Date Submitted by the Author:	21-Feb-2018
Complete List of Authors:	Nguyen, Michael; University of Massachusetts, Geosciences Murphy, Joseph; University of Massachusetts Amherst, Civil & Environmental Engineering Hamlet, Leigh; University of Massachusetts Amherst, Civil & Environmental Engineering Lau, Boris; University of Massachusetts Amherst, Civil & Environmental Engineering, Geosciences

## Environmental Significance

The environmental transformation of sulfidation has been recognized to impact nanoparticle (NP) behavior. Some recent studies have led to the generalization that, during sulfidation, original ligands will be removed, and  $\text{Ag}_2\text{S}$  will become the new ligand shell. For the first time, this study demonstrates that the formation of  $\text{Ag}_2\text{S}$  is ligand-dependent and significantly impacts the consequent mobility and risk of the transformed AgNPs. Due to the selective formation of  $\text{Ag}_2\text{S}$ , not all sulfidized NPs have the same mobilization potential, and therefore it is important to characterize the continuous evolution of specific NP surfaces for better prediction of NP exposure and toxicity.

1  
2  
3  
4 1 **Ligand-Dependent Ag<sub>2</sub>S Formation:**  
5 2 **Changes in Deposition of Silver Nanoparticles with Sulfidation**  
6 3

7  
8  
9 4 Michael L. Nguyen<sup>a</sup>, Joseph A. Murphy<sup>b</sup>, Leigh C. Hamlet<sup>b</sup>, Boris L. T. Lau<sup>ab</sup>  
10

11 5 <sup>a</sup>*Department of Geosciences, University of Massachusetts Amherst, 611 N. Pleasant St., Amherst,*  
12 6 *MA 01002, USA*  
13  
14

15  
16 7 <sup>b</sup>*Department of Civil & Environmental Engineering, University of Massachusetts Amherst, 130*  
17 8 *Natural Resources Road, Amherst, MA 01003, USA*  
18  
19

20 9 Correspondence: Boris L. T. Lau

21 10 E-mail: borislau@umass.edu  
22  
23  
24 11  
25  
26  
27  
28  
29  
30  
31  
32  
33  
34  
35  
36  
37  
38  
39  
40  
41  
42  
43  
44  
45  
46  
47  
48  
49  
50  
51  
52  
53  
54  
55  
56  
57  
58  
59  
60

**Abstract**

The surfaces of nanoparticles (NPs) are continuously evolving as they are exposed to different environmental conditions. Under the same sulfidation condition, silver NPs (AgNPs) are generally considered to undergo the same surface modifications (*i.e.*, removal of original ligands and formation of a new silver sulfide ( $\text{Ag}_2\text{S}$ ) shell). We examined this generalization by studying how different ligands, polyvinylpyrrolidone (PVP) and thiolated polyethylene glycol (PEG), affected 1) the formation of a new  $\text{Ag}_2\text{S}$  shell and 2) the subsequent mobility of these transformed AgNPs. The deposition of PEG-AgNPs onto a silica substrate decreased by a factor of 40 after sulfidation while the deposition of PVP-AgNPs increased by a factor of 15. The decreased deposition of sulfidized PEG-AgNPs was attributed to the removal of PEG and the formation of  $\text{Ag}_2\text{S}$ , which created a more negatively charged surface (-15 mV to -30 mV) and consequently greater electrostatic repulsion with the silica substrate. The increased deposition of sulfidized PVP-AgNPs was suggested to be caused by the removal of PVP and absence of  $\text{Ag}_2\text{S}$ , which decreased steric repulsion with the silica substrate. For the first time, this study revealed the unique abilities of two common polymeric coatings of AgNPs to form  $\text{Ag}_2\text{S}$  during sulfidation and how that  $\text{Ag}_2\text{S}$  determined their subsequent mobility. The results of this communication also highlighted the importance of monitoring the continuous evolution of the NP surface for better prediction of NP exposure and toxicity.

## 31 Introduction

32 The surfaces of environmental nanoparticles (NPs) are continuously evolving along with changes  
33 in its environment (*e.g.*, pH, ionic strength, natural organic matter). Environmental  
34 transformations (*e.g.*, dissolution<sup>1-9</sup> and sulfidation<sup>10-13</sup>) have been shown to significantly impact  
35 the stability and toxicity of NPs. As NPs move through different aquatic environments, they are  
36 exposed daily to different redox conditions and constituents in the environment (*e.g.*, UV  
37 irradiation<sup>14-16</sup> and natural organic matter<sup>16</sup>). These exposures can result in changes in the  
38 composition (and/or steric arrangements) of the “pristine” macromolecules functionalized on the  
39 surfaces of NPs. Since the impact of macromolecular coatings and transformation processes were  
40 both recently reviewed and discussed at length elsewhere,<sup>17,18</sup> it is not the intent of this  
41 introduction to provide a comprehensive overview of these topics but instead to briefly highlight  
42 a subset of the literature that is most relevant to this study.

43 Two pertinent studies by Louie et al.<sup>14,19</sup> demonstrated that NP aggregation could be caused by  
44 photo-induced transformation of polyvinylpyrrolidone (PVP) and thiolated polyethylene glycol  
45 (PEG) coated on gold NPs. These two polymers underwent fundamentally different  
46 transformations. While collapsed PVP was found to persist on gold NPs after UV irradiation, the  
47 methoxy PEG thiol coating was truncated through a chain scission mechanism.<sup>14,19</sup> In addition to  
48 highlighting the importance of characterizing ligand transformation for better prediction of NP  
49 fate and transport, they also stated that the transformation of polymeric NPs 1) cannot be  
50 generalized across different coating types and 2) cannot be assessed using unbound polymers.

51 Partial sulfidation of AgNPs was observed to be highly prevalent in wastewater treatment.<sup>20</sup>  
52 Since sulfide phases are typically much less soluble, sulfidation has been proposed as a natural  
53 detoxification mechanism for metal NPs.<sup>11,12</sup> A common misconception is that metal sulfides are  
54 relatively immobile because of their low solubility; however, the reactivity of metal sulfides  
55 changes at the nanoscale. Despite the low solubility products of silver sulfide (Ag<sub>2</sub>S) ( $K_{sp} = 6.00$   
56  $\times 10^{-51}$ ), large extents of Ag<sub>2</sub>S NP dissolution have been reported.<sup>21</sup> In addition to the intrinsic  
57 toxicity of the metals, metal sulfides are also capable of scavenging other contaminants.<sup>22-27</sup>

58 Overall, findings from recent AgNP sulfidation studies<sup>11,28,29</sup> generally consider that, during  
59 sulfidation, original “pristine” ligands will be removed/modified and Ag<sub>2</sub>S will emerge as the  
60 new ligand shell. This communication examines that generalization by asking the question:

1  
2  
3 61 would Ag<sub>2</sub>S form on the surface of AgNPs regardless of ligand type? In other words, this study  
4 62 sets itself apart by focusing on one important but not well-studied consideration: how different  
5 63 pristine ligands influence 1) the formation of a new Ag<sub>2</sub>S ligand shell and 2) the subsequent  
6 64 deposition of AgNPs on environmental surfaces.  
7  
8  
9

## 10 65 **Results and Discussion**

### 11 66 *Sulfidation Alters AgNP Mobility*

12 67 The deposition of AgNPs (before and after transformation) onto silica substrate was studied  
13 68 through quartz crystal microgravimetry (QCM) and suggested that sulfidation alters AgNP  
14 69 mobility. The mobility of PEG-AgNPs increased after sulfidation as demonstrated by a 40-fold  
15 70 decrease in deposition (Fig. 1A). In contrast, the mobility of PVP-AgNPs decreased after  
16 71 sulfidation as demonstrated by a 15-fold increase in deposition. The trends of increased and  
17 72 decreased mobility for PEG-AgNPs and PVP-AgNPs, respectively, were observed in the absence  
18 73 (Fig. 1A) and presence of natural organic matter (NOM) at different pH conditions (Fig. S1). The  
19 74 deposition behavior of PEG-AgNPs and PVP-AgNPs suggested that the polymeric coating of  
20 75 AgNPs is crucial in determining their subsequent mobility in a sulfidizing environment.  
21  
22  
23  
24  
25  
26  
27  
28  
29

30 76 The zeta potentials of pre- and post-sulfidized PEG-AgNPs and PVP-AgNPs were determined to  
31 77 evaluate the role of electrostatic forces in the observed changes in deposition. Zeta potentials of  
32 78 PEG-AgNPs (Fig. 1B) showed a decrease from -15 mV to -30 mV due to sulfidation. The more  
33 79 negative zeta potentials suggested that 1) the decrease in deposition was likely due to greater  
34 80 electrostatic repulsion between the negatively charged silica substrate and the negatively charged  
35 81 PEG-AgNPs, and 2) sulfidation promoted surface modification of the AgNPs. In contrast, the  
36 82 zeta potential values of PVP-AgNPs (Fig. 1B) showed no significant ( $p>0.05$ ) changes after  
37 83 sulfidation. The similar zeta potentials of PVP-AgNPs before and after sulfidation suggested that  
38 84 1) the change in PVP-AgNP deposition was not due to changes in electrostatic interactions with  
39 85 the silica substrate, and 2) PVP-AgNPs and PEG-AgNPs responded differently to sulfidation, as  
40 86 discussed below.  
41  
42  
43  
44  
45  
46  
47  
48  
49

### 50 87 *Removal of PEG and Ag<sub>2</sub>S Formation*

51 88 The chemical transformations of PEG-AgNPs and PVP-AgNPs were investigated through  
52 89 attenuated total reflection-Fourier transform infrared (ATR-FTIR) and X-ray photoelectron  
53 90 spectroscopy (XPS). The ATR-FTIR spectra of pristine PEG-AgNPs (Fig. 2A) showed three  
54  
55  
56  
57  
58  
59  
60

1  
2  
3 91 distinct bands at 1105 (C-O stretching), 1353 (C-H bending), and 2875 (C-H stretching)  $\text{cm}^{-1}$  and  
4  
5 92 were consistent with the literature.<sup>30</sup> After sulfidation, the three major peaks disappeared  
6  
7 93 completely from the ATR-FTIR spectra, which suggested that PEG was removed during  
8  
9 94 sulfidation. The removal of PEG is further supported by the atomic C % before and after  
10  
11 95 sulfidation (Table S1). After sulfidation, the atomic C % decreased from ~64% to ~19%.  
12  
13 96 The  $\text{Ag}_{3d5/2}$  and  $\text{Ag}_{3d3/2}$  XPS spectra were studied to examine changes in the surface Ag  
14  
15 97 composition. In the pristine state, PEG-AgNPs (Fig. 3A) had binding energies of ~367 eV and  
16  
17 98 ~373 eV, which were attributed to a combination of silver oxide ( $\text{Ag}_2\text{O}$ ), silver carbonate  
18  
19 99 ( $\text{Ag}_2\text{CO}_3$ ), and elemental silver and are consistent with previously reported values.<sup>31,32</sup> After  
20  
21 100 sulfidation, there was a clear shift in the binding energies from ~367 to ~368.2 eV and from  
22  
23 101 ~373 to ~374.2 eV (Fig. 3A). The binding energies of ~368.2 eV and ~374.2 eV in the sulfidized  
24  
25 102 PEG-AgNPs were attributed to silver sulfide and were consistent with XPS analysis of  $\text{Ag}_2\text{S}$   
26  
27 103 particles (Fig. S2). The formation of silver sulfides on PEG-AgNPs supported our  
28  
29 104 complementary characterizations. As the PEG was removed, the AgNP surface was likely  
30  
31 105 exposed to sulfide which allowed for the formation of silver sulfides. The zeta potentials of  
32  
33 106 sulfidized AgNPs were consistent with  $\text{Ag}_2\text{S}$  (-21 to -30 mV). The more negative zeta potential  
34  
35 107 of the sulfidized PEG-AgNPs likely increased the electrostatic repulsion forces between the NPs  
36  
37 108 and silica substrate and resulted in the observed decrease in deposition.

### 35 109 ***Removal of PVP and the Absence of $\text{Ag}_2\text{S}$ Formation***

36  
37 110 The ATR-FTIR spectra of pristine PVP-AgNPs (Fig. 2B) showed four distinct bands at 1289 (C-  
38  
39 111 N stretching), 1424 (C-H bending), 1661 (C=O stretching), and 2954 (C-H stretching)  $\text{cm}^{-1}$  and  
40  
41 112 were consistent with the literature.<sup>33</sup> After sulfidation, the four major peaks remained present but  
42  
43 113 at lower intensities, which suggested some removal of PVP during sulfidation. The removal of  
44  
45 114 PVP was further supported by the atomic C and N % of PVP-AgNPs (Table S1). After  
46  
47 115 sulfidation, the atomic C % decreased from ~71% to ~33% and the atomic N % decreased from  
48  
49 116 ~11 % to ~2 %.

49  
50 117 The  $\text{Ag}_{3d5/2}$  and  $\text{Ag}_{3d3/2}$  XPS spectra of pristine PVP-AgNPs (Fig. 3B) showed that PVP-AgNPs  
51  
52 118 had binding energies similar to those of pristine PEG-AgNPs. The binding energies of 367.4 eV  
53  
54 119 and 373.4 eV were attributed to silver oxide and silver carbonate. In contrast to PEG-AgNPs,  
55  
56 120 there were no observable shifts in binding energies after sulfidation for PVP-AgNPs (Fig. 3B).

1  
2  
3 121 The unchanged binding energies suggested that the removal of PVP did not promote the  
4 122 formation of silver sulfide which was observed for PEG. The removal of PVP and the absence of  
5 123 a Ag<sub>2</sub>S shell likely reduced the steric forces between the PVP-AgNPs and silica substrate and  
6 124 promoted deposition.

7  
8  
9  
10 125 The formation of a new Ag<sub>2</sub>S shell appeared to be dependent on the residual ligand coating. A  
11 126 decrease in atomic C % (Table S1) suggested that both ligands were removed during sulfidation,  
12 127 but the ATR-FTIR spectra (Fig. 2AB) suggested that the extent of removal was ligand-  
13 128 dependent. The ATR-FTIR bands of PEG-AgNPs (Fig. 2A) disappeared while the bands of PVP-  
14 129 AgNPs (Fig. 2B) remained at lower intensities after sulfidation which suggested that more PEG  
15 130 may have been removed relative to PVP. The greater removal of PEG (i.e. lower degree of  
16 131 residual PEG coating; Table S1) likely exposed more of the AgNP surface to sulfide, which  
17 132 promoted the formation of silver sulfides. The remaining bound PVP likely inhibited the  
18 133 exposure of the Ag surface to sulfide and consequently prevented the formation of a Ag<sub>2</sub>S shell.

19  
20  
21  
22  
23  
24  
25  
26 134 One possibility for the difference in the degree of ligand removal may be modification of the  
27 135 PVP due to sulfidation. As observed previously, environmental transformation (UV irradiation)  
28 136 can result in the truncation of ligands through a scission mechanism.<sup>19</sup> In addition, a study by  
29 137 Zhou et al.<sup>34</sup> reported the energetic preference for PVP to bind to Ag {100} facets to be twice  
30 138 that of PEG. For our system, further characterizations are needed to distinguish between the  
31 139 modification and the desorption of the PVP ligand; we hypothesize that it is likely to be a  
32 140 combination of both that contribute to the loss of ligand.

33  
34  
35  
36  
37  
38  
39 141 This communication for the first time revealed the unique importance of two common polymeric  
40 142 coatings of AgNPs, PVP and thiolated PEG, regarding their different ability to form Ag<sub>2</sub>S during  
41 143 sulfidation and how that becomes crucial in determining their subsequent mobility. We found  
42 144 that Ag<sub>2</sub>S formation is ligand-dependent and essential for the persistence of AgNPs after  
43 145 sulfidation. Under our experimental conditions, sulfidation enhanced the immobilization of PVP-  
44 146 AgNPs, therefore decreasing the chances of exposure. For PEG-AgNPs, sulfidation promoted NP  
45 147 mobilization but decreased toxicity due to the formation of Ag<sub>2</sub>S.

46  
47  
48  
49  
50  
51 148 Rational optimization of NP surfaces for specific applications essentially relies on a detailed  
52 149 mechanistic understanding of NP-ligand interactions. Our findings could better inform material  
53 150 chemists as they design and select polymers for stabilization/functionalization of nanomaterials.  
54  
55  
56  
57  
58  
59  
60

1  
2  
3 151 Future work can focus on studying the deposition of NPs under a variety of environmentally  
4 152 relevant conditions (*e.g.*, heterogeneous collector surfaces). The results of this work also  
5 153 highlight the importance of monitoring the continuous evolution of NP surface for better  
6 154 prediction of NP toxicity and exposure.

## 10 155 **Materials and Methods**

### 12 156 *Preparation of AgNPs*

14 157 Spherical PEG- and PVP-capped AgNPs (NanoComposix, San Diego, CA; TEM diameter: 50  
15 158 nm) were used without further purification. The molecular weights of the PEG and PVP capping  
16 159 agents were 5 kDa and 40 kDa, respectively. The NP stock solutions were diluted from 5000  
17 160 mg/L (PEG-AgNPs) and 1000 mg/L (PVP-AgNPs) to 100 mg/L with ultrapure deionized water  
18 161 (Milli-Q™, 18.2 mΩ) to obtain a final particle concentration of  $1.24 \times 10^{10}$  particles/L. Filtered  
19 162 (0.20 μm) stock solutions of NaNO<sub>3</sub> and HEPES were used to adjust the final electrolyte  
20 163 concentration to 50 mM NaNO<sub>3</sub> and 1 mM HEPES. The final pH of the suspensions was  
21 164 adjusted to  $5.0 \pm 0.2$  and  $7.0 \pm 0.2$ .

22 165 Unfractionated Suwanee River NOM (International Humic Substances Society) was dissolved in  
23 166 ultrapure deionized water and filtered (0.20 μm). The organic carbon content of the NOM stock  
24 167 solution was determined through total organic carbon analysis (Shimadzu TOCV; Kyoto, Japan).  
25 168 All stock suspensions and solutions were stored in the dark at 4°C.

26 169 The sulfidation of AgNPs was conducted using sodium sulfide (Na<sub>2</sub>S) in the manner described  
27 170 by Levard et al. (2011).<sup>11</sup> The AgNP suspensions were mixed with Na<sub>2</sub>S in the presence of 40  
28 171 mg/L NOM to obtain a S/Ag ratio of 1.079. The suspensions were mixed in the dark for 24 hr.  
29 172 After 24 hr, the suspensions were centrifuged at 3700 G for 25 min, and the supernatant was  
30 173 decanted. The NP suspensions were washed at least two times with ultrapure deionized water to  
31 174 remove excess sulfide and NOM. After the final washing step, ultrapure deionized water was  
32 175 added to the suspension to reach the desired particle concentration. The pristine and sulfidized  
33 176 NPs are suspended in the same solution chemistry for all experiments and characterizations.

### 35 177 *Deposition of AgNPs*

36 178 The real-time deposition of pristine and sulfidized AgNPs onto silica substrate (Q-Sense AB, Q-  
37 179 Sense AB, Gothenburg, Sweden) were monitored and quantified through QCM. The deposition  
38 180 extent, in ng/cm<sup>2</sup>, was determined by measuring oscillation frequency changes in the quartz

1  
2  
3 181 crystal (due to NP deposition) and relating those changes to mass changes through the Sauerbrey  
4  
5 182 relationship. The deposition experiments were conducted in the same solution chemistry as  
6  
7 183 described above, at  $25 \pm 0.2$  °C, and in the absence and presence of NOM (5 mg/L). The  
8  
9 184 deposition experiments were repeated at least three times; the average values and standard  
10  
11 185 deviations (error bars) are reported.

### 12 186 ***Characterization of AgNPs***

14 187 The electrophoretic mobility of the pristine and sulfidized AgNPs were measured at  $25 \pm 0.2$  °C  
15  
16 188 using a Malvern Zetasizer NS (Worcestershire, UK). The zeta potential value was derived from  
17  
18 189 the electrophoretic mobility using the Smoluchowski equation. In addition to the pristine and  
19  
20 190 sulfidized AgNPs, the zeta potential of Ag<sub>2</sub>S (Sigma-Aldrich) was measured. The Ag<sub>2</sub>S particles  
21  
22 191 were ground by mortar and pestle, suspended in ultrapure deionized water at the solution  
23  
24 192 chemistry described above, and filtered (0.45 μm) prior to measurement. All reported values  
25  
26 193 represented the average of at least three replicates and included a minimum of thirteen runs.

27 194 The ATR-FTIR analysis was conducted on pre- and post-sulfidized NP samples to characterize  
28  
29 195 changes in ligand-NP interactions. All ATR-FTIR spectra were collected using a Perkin-Elmer  
30  
31 196 Spectrum One FTIR spectrometer, equipped with a lithium tantalate (LiTaO<sub>3</sub>) detector and a  
32  
33 197 one-reflection horizontal ATR accessory with a diamond/ZnSe crystal (Shelton, CT).

34 198 Approximately 30 μL of sample were drop-casted onto the crystal and air dried prior to spectra  
35  
36 199 collection. Atmospheric background spectra were subtracted from the samples and baseline  
37  
38 200 correction was completed through the Spectrum software. All spectra were obtained by  
39  
40 201 collecting 250 scans with a spectral resolution of 4 cm<sup>-1</sup> between 650 and 4000 cm<sup>-1</sup> at a scan  
41  
42 202 speed of 1.0 cm/s. Measurements were replicated at least two times.

43 203 The XPS analysis was used to examine changes in the AgNP surface chemistry before and after  
44  
45 204 sulfidation. Prior to XPS analysis, samples were deposited onto a glass slide and air-dried.  
46  
47 205 Spectra were collected on a Physical Electronics Quantum 2000 Scanning ESCA Microprobe,  
48  
49 206 and analyzed using PHI's software based on MATLAB, MultiPak v.9.0. An internal metal  
50  
51 207 standard (*i.e.* Ag) was used for the standardization of the spectra. Specifically, the peak at 368.3  
52  
53 208 eV for the Ag<sub>2</sub>S (Sigma-Aldrich) was used to determine if shifts in the sample spectra were  
54  
55 209 needed.

### 56 210 **Conflicts of Interest**

57  
58  
59  
60

1  
2  
3 211 There are no conflicts to declare.  
4

## 5 212 **Acknowledgments**

6 213 The authors would like to thank Mr. Jacob Hirsch for technical support with the XPS  
7  
8 214 measurements and Dr. Baoshan Xing's group for granting us access to their ATR-FTIR. This  
9  
10 215 research was financially supported by the US National Science Foundation (CBET 1336167).  
11

## 12 216 **Supplementary Information**

13 217 The Supplementary Information includes the deposition data of pristine and sulfidized PEG- and  
14  
15 218 PVP-AgNPs in the presence of NOM, the atomic C and N % of pristine and sulfidized PEG- and  
16  
17 219 PVP-AgNPs, and the Ag<sub>3d5/2</sub> and Ag<sub>3d3/2</sub> XPS spectra of Ag<sub>2</sub>S.  
18

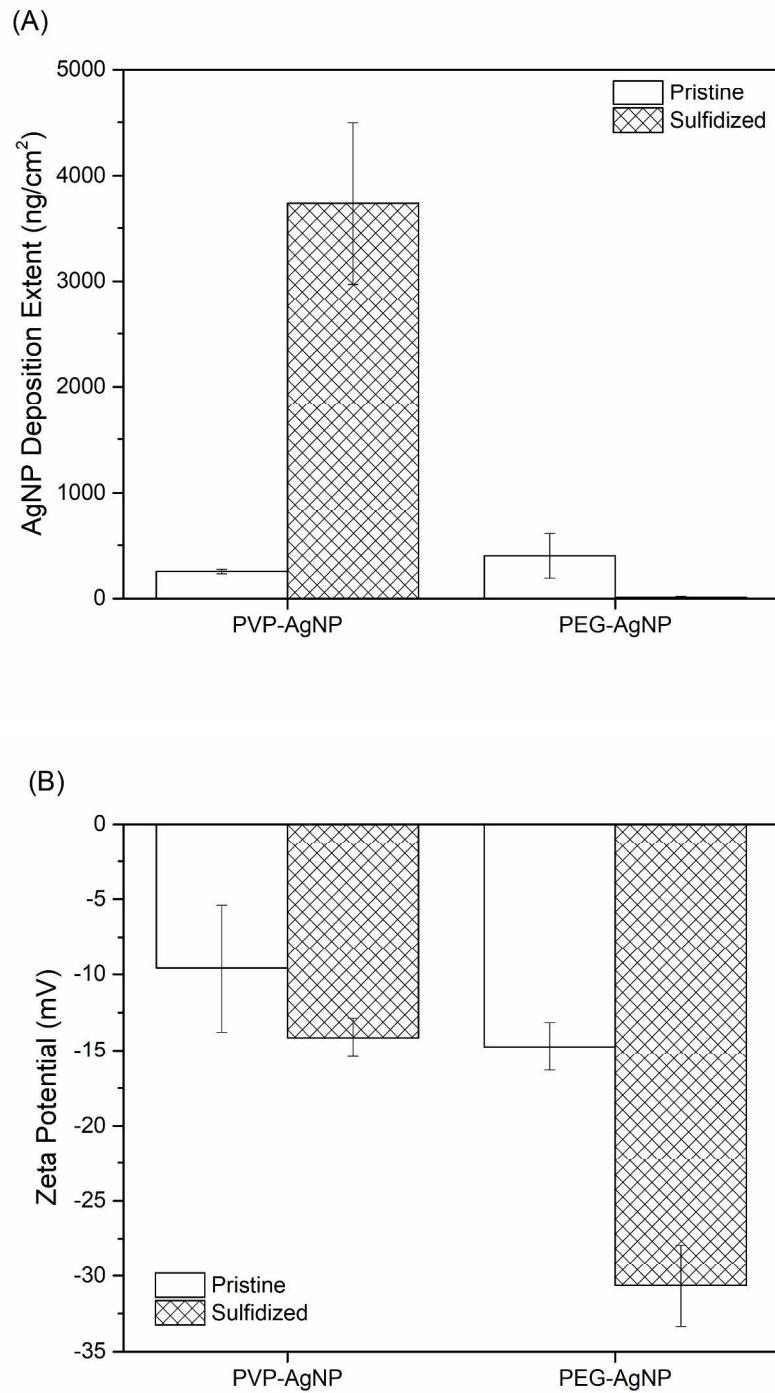
## 19 220 **References**

- 20 221 (1) Ma, R.; Levard, C.; Marinakos, S. M.; Cheng, Y.; Liu, J.; Michel, F. M.; Brown, G. E.;  
21  
22 222 Lowry, G. V. Size-Controlled Dissolution of Organic-Coated Silver Nanoparticles.  
23  
24 223 *Environ. Sci. Technol.* **2012**, *46* (2), 752–759 DOI: 10.1021/es201686j.  
25  
26 224 (2) Li, X.; Lenhart, J. J.; Walker, H. W. Dissolution-accompanied aggregation kinetics of  
27  
28 225 silver nanoparticles. *Langmuir* **2010**, *26* (22), 16690–16698 DOI: 10.1021/la101768n.  
29  
30 226 (3) Li, X.; Lenhart, J. J. Aggregation and dissolution of silver nanoparticles in natural surface  
31  
32 227 water. *Environ. Sci. Technol.* **2012**, *46* (10), 5378–5386 DOI: 10.1021/es204531y.  
33  
34 228 (4) Li, X.; Lenhart, J. J.; Walker, H. W. Aggregation kinetics and dissolution of coated silver  
35  
36 229 nanoparticles. *Langmuir* **2012**, *28* (2), 1095–1104 DOI: 10.1021/la202328n.  
37  
38 230 (5) Elzey, S.; Grassian, V. H. Agglomeration, isolation and dissolution of commercially  
39  
40 231 manufactured silver nanoparticles in aqueous environments. *J. Nanoparticle Res.* **2010**, *12*  
41  
42 232 (5), 1945–1958 DOI: 10.1007/s11051-009-9783-y.  
43  
44 233 (6) Unrine, J. M.; Colman, B. P.; Bone, A. J.; Gondikas, A. P.; Matson, C. W. Biotic and  
45  
46 234 abiotic interactions in aquatic microcosms determine fate and toxicity of ag nanoparticles.  
47  
48 235 Part 1. Aggregation and dissolution. *Environ. Sci. Technol.* **2012**, *46* (13), 6915–6924  
49  
50 236 DOI: 10.1021/es204682q.  
51  
52 237 (7) Zook, J. M.; Halter, M. D.; Cleveland, D.; Long, S. E. Disentangling the effects of  
53  
54 238 polymer coatings on silver nanoparticle agglomeration, dissolution, and toxicity to  
55  
56 239 determine mechanisms of nanotoxicity. *J. Nanoparticle Res.* **2012**, *14* (10), 1–9 DOI:  
57  
58 240 10.1007/s11051-012-1165-1.  
59  
60 241 (8) Kittler, S.; Greulich, C.; Diendorf, J.; Köller, M.; Epple, M. Toxicity of silver

- nanoparticles increases during storage because of slow dissolution under release of silver ions. *Chem. Mater.* **2010**, *22* (16), 4548–4554 DOI: 10.1021/cm100023p.
- (9) He, D.; Dorantes-Aranda, J. J.; Waite, T. D. Silver nanoparticle-algae interactions: Oxidative dissolution, reactive oxygen species generation and synergistic toxic effects. *Environ. Sci. Technol.* **2012**, *46* (16), 8731–8738 DOI: 10.1021/es300588a.
- (10) Lowry, G. V.; Espinasse, B. P.; Badireddy, A. R.; Richardson, C. J.; Reinsch, B. C.; Bryant, L. D.; Bone, A. J.; Deonaraine, A.; Chae, S.; Therezien, M.; et al. Long-Term Transformation and Fate of Manufactured Ag Nanoparticles in a Simulated Large Scale Freshwater Emergent Wetland. *Environ. Sci. Technol.* **2012**, *46* (13), 7027–7036 DOI: 10.1021/es204608d.
- (11) Levard, C.; Reinsch, B. C.; Michel, F. M.; Oumahi, C.; Lowry, G. V.; Brown, G. E. Sulfidation processes of PVP-coated silver nanoparticles in aqueous solution: Impact on dissolution rate. *Environ. Sci. Technol.* **2011**, *45* (12), 5260–5266 DOI: 10.1021/es2007758.
- (12) Reinsch, B. C.; Levard, C.; Li, Z.; Ma, R.; Wise, A.; Gregory, K. B.; Brown, G. E.; Lowry, G. V. Sulfidation of silver nanoparticles decreases *Escherichia coli* growth inhibition. *Environ. Sci. Technol.* **2012**, *46* (13), 6992–7000 DOI: 10.1021/es203732x.
- (13) Liu, J.; Pennell, K. G.; Hurt, R. H. Kinetics and mechanisms of nanosilver oxysulfidation. *Environ. Sci. Technol.* **2011**, *45* (17), 7345–7353 DOI: 10.1021/es201539s.
- (14) Louie, S. M.; Gorham, J. M.; McGivney, E. A.; Liu, J.; Gregory, K. B.; Hackley, V. A. Photochemical transformations of thiolated polyethylene glycol coatings on gold nanoparticles. *Environ. Sci. Nano* **2016**, *3* (5), 1090–1102 DOI: 10.1039/C6EN00141F.
- (15) Mittelman, A. M.; Fortner, J. D.; Pennell, K. D.; Lifia, J.; Amal, R.; Sun, H.; Tam, P. K.; Chiu, J.; Che, C.; Labille, J.; et al. Effects of ultraviolet light on silver nanoparticle mobility and dissolution. *Environ. Sci. Nano* **2015**, *2* (6), 683–691 DOI: 10.1039/C5EN00145E.
- (16) Hou, W. C.; Stuart, B.; Howes, R.; Zepp, R. G. Sunlight-driven reduction of silver ions by natural organic matter: Formation and transformation of silver nanoparticles. *Environ. Sci. Technol.* **2013**, *47* (14), 7713–7721 DOI: 10.1021/es400802w.
- (17) Levard, C.; Hotze, E. M.; Lowry, G. V.; Brown, G. E. Environmental Transformations of Silver Nanoparticles: Impact on Stability and Toxicity. *Environ. Sci. Technol.* **2012**, *46*

- 1  
2  
3 273 (13), 6900–6914 DOI: 10.1021/es2037405.
- 4  
5 274 (18) Louie, S. M.; Tilton, R. D.; Lowry, G. V. Critical review: impacts of macromolecular  
6  
7 275 coatings on critical physicochemical processes controlling environmental fate of  
8  
9 276 nanomaterials. *Environ. Sci. Nano* **2016**, *3* (2), 283–310 DOI: 10.1039/C5EN00104H.
- 10  
11 277 (19) Louie, S. M.; Gorham, J. M.; Tan, J.; Hackley, V. A. Ultraviolet photo-oxidation of  
12  
13 278 polyvinylpyrrolidone (PVP) coatings on gold nanoparticles. *Environ. Sci. Nano* **2017**, *4*  
14  
15 279 (9), 1866–1875 DOI: 10.1039/C7EN00411G.
- 16  
17 280 (20) Kaegi, R.; Voegelin, A.; Ort, C.; Sinnet, B.; Thalmann, B.; Krismer, J.; Hagendorfer, H.;  
18  
19 281 Elumelu, M.; Mueller, E. Fate and transformation of silver nanoparticles in urban  
20  
21 282 wastewater systems. *Water Res.* **2013**, *47* (12), 3866–3877 DOI:  
22  
23 283 10.1016/j.watres.2012.11.060.
- 24  
25 284 (21) Li, L.; Xu, Z.; Wimmer, A.; Tian, Q.; Wang, X. New Insights into the Stability of Silver  
26  
27 285 Sulfide Nanoparticles in Surface Water: Dissolution through Hypochlorite Oxidation.  
28  
29 286 *Environ. Sci. Technol.* **2017**, *51* (14), 7920–7927 DOI: 10.1021/acs.est.7b01738.
- 30  
31 287 (22) Aubriet, H.; Humbert, B.; Perdicakis, M. Interaction of U(VI) with pyrite, galena and their  
32  
33 288 mixtures: a theoretical and multitechnique approach. *Radiochim. Acta* **2006**, *94* (9–11)  
34  
35 289 DOI: 10.1524/ract.2006.94.9-11.657.
- 36  
37 290 (23) Tauson, V. L.; Parkhomenko, I. Y.; Babkin, D. N.; Men'shikov, V. I.; Lustenberg, E. E.  
38  
39 291 Cadmium and mercury uptake by galena crystals under hydrothermal growth: A  
40  
41 292 spectroscopic and element thermo-release atomic absorption study. *Eur. J. Mineral.* **2005**,  
42  
43 293 *17* (4), 599–610 DOI: 10.1127/0935-1221/2005/0017-0599.
- 44  
45 294 (24) Genin, F.; Alnot, M.; Ehrhardt, J. J. Interaction of vapours of mercury with PbS(001): a  
46  
47 295 study by X-ray photoelectron spectroscopy, RHEED and X-ray absorption spectroscopy.  
48  
49 296 *Appl. Surf. Sci.* **2001**, *173* (1–2), 44–53 DOI: 10.1016/S0169-4332(00)00874-6.
- 50  
51 297 (25) Cao, Z.; Liu, X.; Xu, J.; Zhang, J.; Yang, Y.; Zhou, J.; Xu, X.; Lowry, G. V. Removal of  
52  
53 298 Antibiotic Florfenicol by Sulfide-Modified Nanoscale Zero-Valent Iron. *Environ. Sci.*  
54  
55 299 *Technol.* **2017**, *51* (19), 11269–11277 DOI: 10.1021/acs.est.7b02480.
- 56  
57 300 (26) Gong, Y.; Liu, Y.; Xiong, Z.; Zhao, D. Immobilization of Mercury by Carboxymethyl  
58  
59 301 Cellulose Stabilized Iron Sulfide Nanoparticles: Reaction Mechanisms and Effects of  
60  
302 Stabilizer and Water Chemistry. *Environ. Sci. Technol.* **2014**, *48* (7), 3986–3994 DOI:  
303  
10.1021/es404418a.

- 1  
2  
3 304 (27) Su, Y.; Adeleye, A. S.; Keller, A. A.; Huang, Y.; Dai, C.; Zhou, X.; Zhang, Y. Magnetic  
4 305 sulfide-modified nanoscale zerovalent iron (S-nZVI) for dissolved metal ion removal.  
5 306 *Water Res.* **2015**, *74*, 47–57 DOI: 10.1016/j.watres.2015.02.004.  
6  
7  
8 307 (28) Zhu, T.; Lawler, D. F.; Chen, Y.; Lau, B. L. T. Effects of natural organic matter and  
9 308 sulfidation on the flocculation and filtration of silver nanoparticles. *Environ. Sci. Nano*  
10 309 **2016**, *3* (6), 1436–1446 DOI: 10.1039/C6EN00266H.  
11  
12  
13 310 (29) Thalmann, B.; Voegelin, A.; Morgenroth, E.; Kaegi, R. Effect of humic acid on the  
14 311 kinetics of silver nanoparticle sulfidation. *Environ. Sci. Nano* **2016**, *3* (1), 203–212 DOI:  
15 312 10.1039/C5EN00209E.  
16  
17  
18 313 (30) Shameli, K.; Ahmad, M. Bin; Jazayeri, S. D.; Sedaghat, S.; Shabanzadeh, P.; Jahangirian,  
19 314 H.; Mahdavi, M.; Abdollahi, Y. Synthesis and characterization of polyethylene glycol  
20 315 mediated silver nanoparticles by the green method. *Int. J. Mol. Sci.* **2012**, *13* (6), 6639–  
21 316 6650 DOI: 10.3390/ijms13066639.  
22  
23  
24 317 (31) Prieto, P.; Nistor, V.; Nouneh, K.; Oyama, M.; Abd-Lefdil, M.; Díaz, R. XPS study of  
25 318 silver, nickel and bimetallic silver–nickel nanoparticles prepared by seed-mediated  
26 319 growth. *Appl. Surf. Sci.* **2012**, *258* (22), 8807–8813 DOI: 10.1016/j.apsusc.2012.05.095.  
27  
28  
29 320 (32) Sumesh, E.; Bootharaju, M. S.; Anshup; Pradeep, T. A practical silver nanoparticle-based  
30 321 adsorbent for the removal of Hg<sup>2+</sup> from water. *J. Hazard. Mater.* **2011**, *189* (1–2), 450–  
31 322 457 DOI: 10.1016/j.jhazmat.2011.02.061.  
32  
33  
34 323 (33) Pettibone, J. M.; Liu, J. In Situ Methods for Monitoring Silver Nanoparticle Sulfidation in  
35 324 Simulated Waters. *Environ. Sci. Technol.* **2016**, *50* (20), 11145–11153 DOI:  
36 325 10.1021/acs.est.6b03023.  
37  
38  
39 326 (34) Zhou, Y.; Saidi, W. A.; Fichthorn, K. A. Comparison of the Binding of  
40 327 Polyvinylpyrrolidone and Polyethylene Oxide to Ag Surfaces: Elements of a Successful  
41 328 Structure-Directing Agent. *J. Phys. Chem. C* **2013**, *117* (21), 11444–11448 DOI:  
42 329 10.1021/jp403318h.  
43  
44  
45  
46  
47  
48 330  
49 331  
50  
51  
52  
53  
54  
55  
56  
57  
58  
59  
60

332 **Figures**

333

334

335 **Figure 1.** The (A) deposition and (B) zeta potential of pristine and sulfidized PVP- and PEG-  
336 capped AgNPs onto QCM silica sensors in 5 mM NaNO<sub>3</sub> (pH 7). Error bars represent the  
337 standard deviation of at least three replicate experiments.

338

339

340

341

342

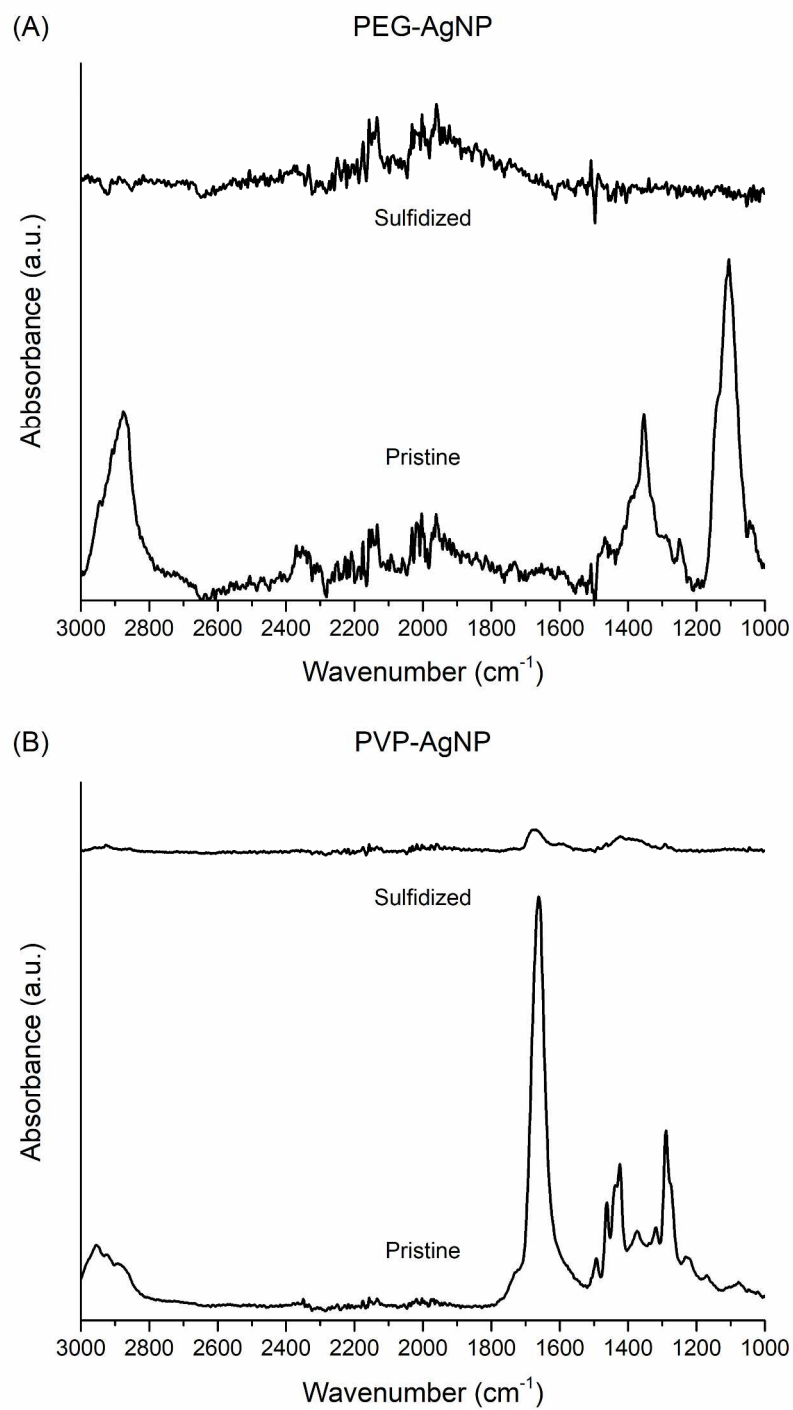
343

344

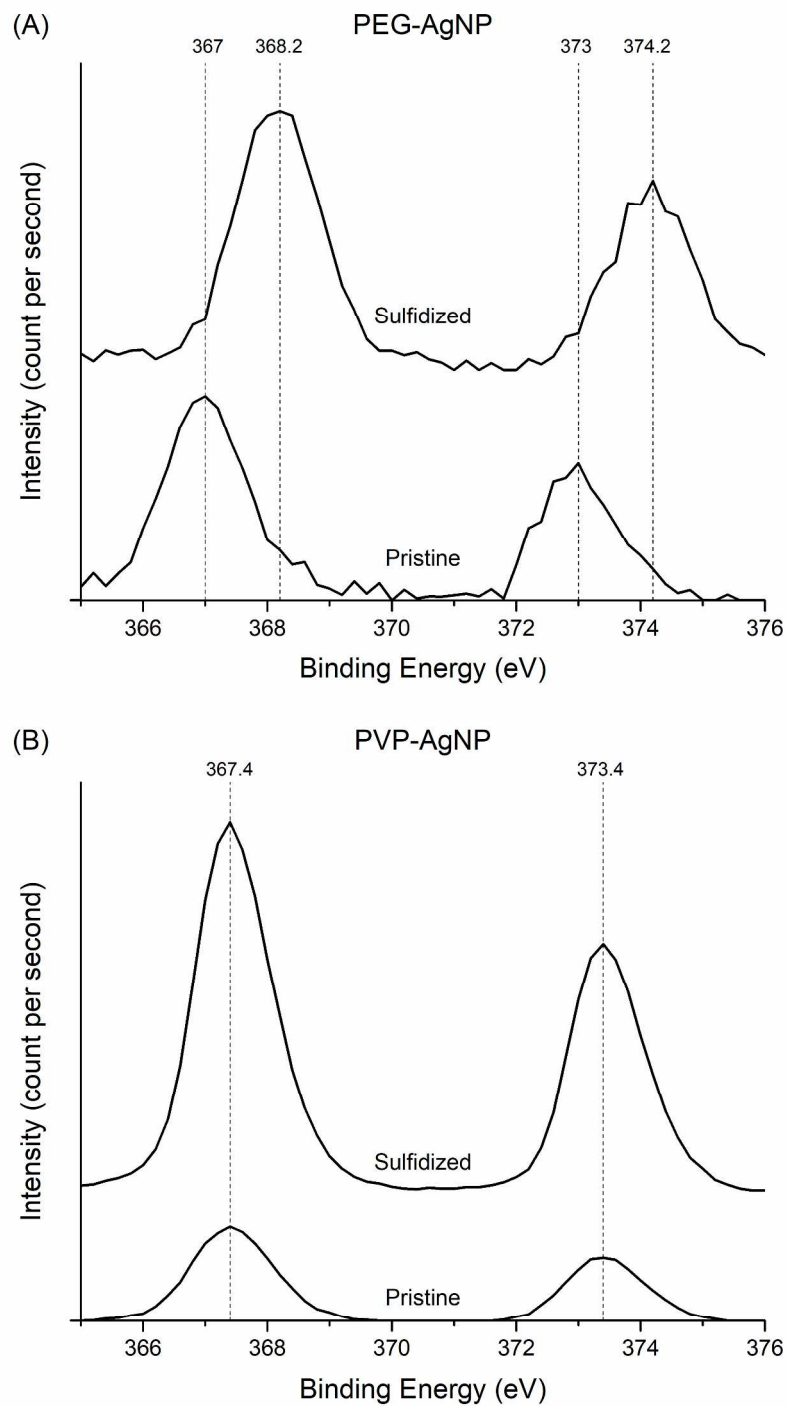
345

1  
2  
3  
4  
5  
6  
7  
8  
9  
10  
11  
12  
13  
14  
15  
16  
17  
18  
19  
20  
21  
22  
23  
24  
25  
26  
27  
28  
29  
30  
31  
32  
33  
34  
35  
36  
37  
38  
39  
40  
41  
42  
43  
44  
45  
46  
47  
48  
49  
50  
51  
52  
53  
54  
55  
56  
57  
58  
59  
60

339



341  
342 **Figure 2.** The ATR-FTIR spectra of (A) PEG- and (B) PVP-capped AgNPs in the pristine and  
343 sulfidized states.



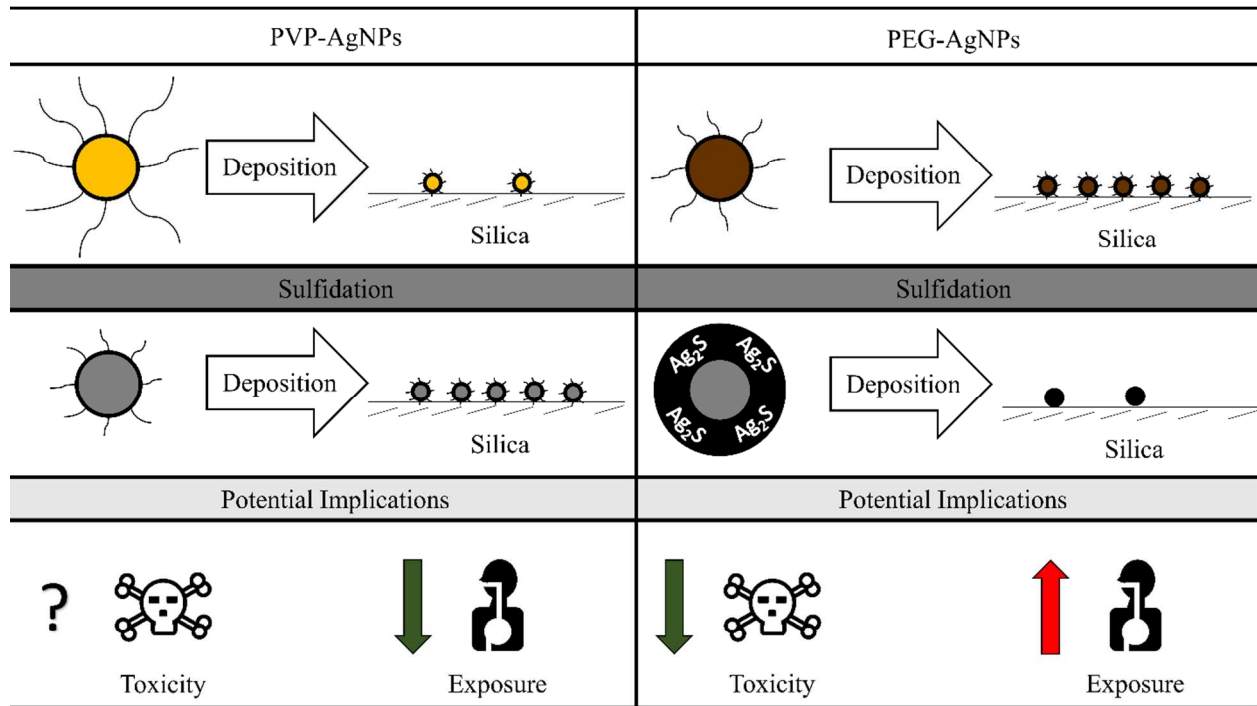
346

347

348 **Figure 3.** The  $\text{Ag}_{3d_{5/2}}$  and  $\text{Ag}_{3d_{3/2}}$  XPS spectra of (A) PEG- and (B) PVP-coated AgNPs in the  
349 pristine and sulfidized states.

350

TOC Art



The formation of silver sulfide on the surface of silver nanoparticles is ligand-dependent and is essential for their persistence after sulfidation.

1  
2  
3  
4  
5  
6  
7  
8  
9  
10  
11  
12  
13  
14  
15  
16  
17  
18  
19  
20  
21  
22  
23  
24  
25  
26  
27  
28  
29  
30  
31  
32  
33  
34  
35  
36  
37  
38  
39  
40  
41  
42  
43  
44  
45  
46  
47  
48  
49  
50  
51  
52  
53  
54  
55  
56  
57  
58  
59  
60